inter-noise 2021
1–5 August | Washington, DC

# Using Inverse Transient Statistical Energy Analysis to determine the transient power input from a heavy impact on floating floors

Susumu HIRAKAWA[1,2]
Acoustics Research Unit, School of Architecture, University of Liverpool
Liverpool L697ZN United Kingdom.

Carl HOPKINS[3]
Acoustics Research Unit, School of Architecture, University of Liverpool

**ABSTRACT**

*To assess heavy impacts on heavyweight floors, it is necessary to be able to predict the Fast-time weighted maximum sound pressure ($L_{p,Fmax}$) in a receiving room. For excitation directly on the heavyweight floor this can be carried out using Transient Statistical Energy Analysis (TSEA) in a predictive mode. However, the performance of floating floors is not always possible to accurately predict, hence an inverse approach to TSEA is developed using laboratory measurements, referred to as ITSEA, to determine the transient power that is determined by the floating floor. This paper predicts $L_{p,Fmax}$ in a receiving room using TSEA with normalized transient power input determined by ITSEA. A comparison is made against measurements conducted in two test facilities with and without floating floors (full-size and small samples) on a concrete base floor which showed reasonable agreement (typically <5dB) for both one-third octave bands and octave bands.*

## 1. INTRODUCTION

The measurement of impact sound insulation in buildings due to heavy impacts on floors is described in standards [1–4] which use standardized excitation sources such as a rubber ball or bang machine. The standards require the Fast time-weighted maximum sound pressure level, $L_{p,Fmax}$ in the room under the floor that is excited by the heavy impact sources. However, there are few validated models available to predict $L_{p,Fmax}$ due to heavy impact sources.

To allow prediction of $L_{p,Fmax}$ from any form of heavy impact source excited in heavyweight buildings, Robinson and Hopkins [5,6] showed that Transient Statistical Energy Analysis (TSEA) can be used to predict from the combination of direct and flanking paths. They subsequently showed that TSEA can be used to predict $L_{p,Fmax}$ due to excitation of a concrete base floor that is directly excited by the rubber ball or human footsteps [7].

In a real building where there is usually a floor finish (e.g., floating floor) on top of the base floor to provide insulation against light impacts such as footsteps from walkers in shoes, as well as heavy impacts such as from children running or jumping. Therefore, it is necessary to identify and experimentally validate a new approach to incorporate floating floors in TSEA models of heavyweight

[1] Current affiliation: Building Research Institute, 1 Tachihara, Tsukuba, Japan
[2] sh@kenken.go.jp
[3] carl.hopkins@liverpool.ac.uk

buildings. Hirakawa and Hopkins proposed an inverse form of TSEA (ITSEA) to experimentally determine the transient power input for the combination of the heavy impact source and floor, and the combination of the heavy impact source and floating floor. For small, idealized version of floating floor system (i.e. mass-spring sytems) that would fit on top of a force plate in order to measure the blocked force there was close agreement between ITSEA and force plate measurements [8].

In this paper, the TSEA prediction model was used with normalized transient power inputs that were determined with ITSEA to compare the predicted and measured $L_{p,Fmax}$ inside the receiving room of two test facilities. These facilities had a concrete separating floor with and without floating floor and the heavy impact sources were a rubber ball and bang machine.

## 2. INVERSE TRANSIENT STATISTICAL ENERGY ANALYSIS (ITSEA)

ITSEA is used to determine the transient power input into the source subsystem, $i$, in a system comprising of $X$ subsystems shown in Eq.(1)

$$W_{\text{in,ITSEA},i} = \frac{1}{N}\sum_{n=1}^{N} \frac{\left(E_i(t_{n+1}) - E_i(t_n)\right)}{\Delta t} - \left(\sum_{j\neq i}^{X} \omega\eta_{ji}E_j(t_n) - \omega\eta_i E_i(t_n)\right) \quad (1)$$

where $N$ is the integer number of time steps between 0 s and $t_{\text{peak}}$.

Use of Eq. (1) requires the time-varying, mean-square energy on the source subsystem and all subsystems directly connected to the source subsystem, all the CLFs that directly transfer energy from other subsystems to the source subsystem. It is experimentally demanding to measure time-varying, mean-square energy on the source subsystem and all the subsystems that are directly connected to it. Thus, it is simpler if ITSEA only considers the source subsystem. This allows Eq. (1) to be simplified to

$$W_{\text{in,ITSEA},i} \approx \frac{1}{N}\sum_{n=1}^{N} \left[\frac{\left(E_i(t_{n+1}) - E_i(t_n)\right)}{\Delta t} + \omega\eta_i E_i(t_n)\right] \quad (2)$$

Determining the transient power input to be injected into a TSEA model during the time that the force is applied requires that the values obtained from Eq. (2) are modified to give the normalised transient power input using

$$W'_{\text{in,ITSEA},i} = \frac{t_{\text{peak}}}{t_{\text{input\_duration}}} W_{\text{in,ITSEA},i} \quad (3)$$

where $t_{\text{peak}}$ is the time at which the first peak occurs in the mean-square velocity, and $t_{\text{input\_duration}}$ is the actual duration of the force pulse. For a heavy impact directly onto the base floor, $t_{\text{input\_duration}}$ can be determined from force plate measurements, but it is not possible to use the force plate to determine $t_{\text{input\_duration}}$ for a heavy impact on a full-size floating floor.

## 3. TEST FACILITIES

Figure 1 (left) shows test facility A, a vertical transmission suite (BRE, UK) with suppressed flanking transmission. This has a 140mm solid concrete base floor (345kg/m$^2$) as prescribed in ISO 10140-5:2010+A1 2014 for the measurement of the improvement of impact sound insulation from floor coverings. The base floor dimensions are 4.19m × 3.61m, and the lower and upper rooms each have a volume of ≈50m$^3$. The lower room is the receiving room which is formed by four 215mm solid masonry walls (430kg/m$^2$) that are built off a 300mm solid concrete ground floor (660kg/m$^2$). Flanking transmission is suppressed inside this lower room with independent plasterboard linings on the walls and a floating screed floor. The upper room is formed by lightweight plasterboard stud walls and a plasterboard ceiling. The dimensions of test facility A in terms of the subsystems used in the TSEA model are summarised in Table.1 where Room 2 is the receiving room and Floor 3 is the 140mm base floor (fundamental frequency is 32Hz).

Figure 1 (right) shows the test facility B. It is a stand-alone test room (LH, South Korea) with a 210mm solid concrete base floor (462kg/m$^2$) that is commonly used in Korean dwellings. The base floor dimensions are 4.76m × 4.10m (fundamental frequency is 37.4Hz). The receiving room has a volume of ≈50m$^3$. The facility has one glazed façade, three 200mm concrete walls without any wall linings, and a 300mm ground floor without a floating floor. The properties and dimensions of test facility B are given in Table.2 for the two subsystems used in the TSEA model. Due to the absence of information on the other walls and floors it was assumed that flanking transmission was negligible.

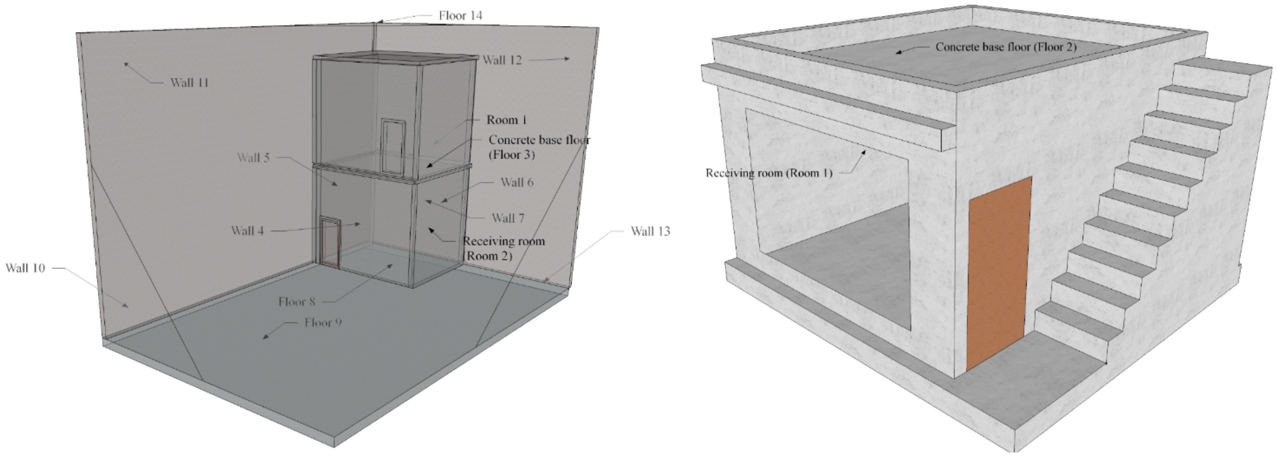


*Figure 1. Test facility A (left) and test facility B (right)*

In test facility B, the floating floor is on top of the base floor the Ondol system that is commonly used in South Korea. The rigid walking surface is 40mm lightweight concrete (27.6kg/m$^2$) bonded directly to 40mm mortar (72kg/m$^2$) on a resilient material of 30mm EPS with dynamic stiffness per unit area of 20MN/m$^3$. The mass-spring resonance frequency is calculated to be 71Hz.

The locally reacting mass-spring systems are introduced in order to represent a highly idealised version of a floating floor. Their small size enables the blocked force due to the combination of the rubber ball and floating floor to be measured on the force plate. Each mass-spring system comprises a 20mm thick steel plate (200mm × 200mm) on top of a different resilient material shown in Figure.2. The parameters of the locally reacting mass-spring systems are given in Table 3.

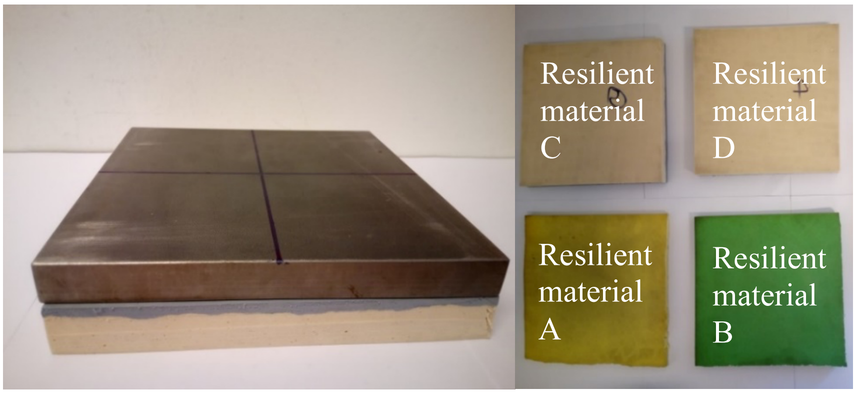


*Figure 2. Resilient material and steel plate (locally reacting mass-spring systems) (left), and tested materials (A, B, C, D and E) (right).*

*Table 1. Test facility A: Properties of the rooms, walls and floors.*

| Subsystem | $L_x$ (m) | $L_y$ (m) | $L_z$ (m) | $U$ (m) | $S$ (m) | $\rho_s$ (kg/m$^2$) | $c_L$ (m) | $\eta_{ii}$ (-) |
|---|---|---|---|---|---|---|---|---|
| Room 1 | 4.18 | 3.61 | 3.51 | - | - | - | - | - |
| **Room 2** | **3.92** | **3.33** | **3.91** | **-** | **-** | **-** | **-** | **-** |
| Subsystem | $L_x$ (m) | $L_y$ (m) | $h$ (m) | $U$ (m) | $S$ (m) | $\rho_s$ (kg/m$^2$) | $c_L$ (m) | $\eta_{ii}$ (-) |
| **Floor 3** | **4.19** | **3.61** | **0.14** | **15.58** | **15.09** | **345.4** | **3856** | **0.005** |
| Wall 4 | 3.61 | 3.91 | 0.215 | 15.04 | 12.22 | 430 | 3200 | 0.01 |
| Wall 5 | 4.19 | 3.91 | 0.215 | 16.18 | 16.34 | 430 | 3200 | 0.01 |
| Wall 6 | 3.61 | 3.91 | 0.215 | 15.04 | 14.12 | 430 | 3200 | 0.01 |
| Wall 7 | 4.19 | 3.91 | 0.3 | 16.18 | 16.34 | 430 | 3200 | 0.01 |
| Floor 8 | 4.19 | 3.61 | 0.3 | 15.58 | 15.09 | 660 | 3680 | 0.005 |
| Floor 9 | 14.03 | 9.15 | 0.2 | 46.00 | 113.28 | 660 | 3680 | measured |
| Wall 10 | 9.76 | 9.15 | 0.2 | 37.82 | 89.4 | 440 | 3680 | 0.005 |
| Wall 11 | 14.03 | 9.76 | 0.2 | 47.58 | 136.93 | 1088 | 3680 | 0.005 |
| Wall 12 | 9.76 | 9.15 | 0.2 | 37.82 | 89.4 | 440 | 3680 | 0.005 |
| Wall 13 | 14.03 | 9.76 | 0.2 | 47.58 | 136.93 | 440 | 3680 | 0.005 |
| Floor 14 | 14.03 | 9.15 | 0.2 | 46.00 | 128.37 | 440 | 3680 | 0.005 |

*Table 2. Test facility B: Properties of the room and floor subsystems*

| **Subsystem** | **$L_x$ (m)** | **$L_y$ (m)** | **$L_z$ (m)** | - | - | - | - | - |
|---|---|---|---|---|---|---|---|---|
| **Room 1** | 4.78 | 4.10 | 2.59 | - | - | - | - | - |
| **Subsystem** | **$L_x$ (m)** | **$L_y$ (m)** | **$h$ (m)** | ***$U$ (m)*** | ***$S$ (m)*** | ***$\rho_s$ (kg/m$^2$)*** | ***$c_L$ (m)*** | ***$\eta_{ii}$ (-)*** |
| **Floor 2** | 4.78 | 4.10 | 0.21 | 17.76 | 19.6 | 3200 | 3800 | 0.005 |

*Table 3. Parameters describing the mass-spring systems. Dynamic stiffness and loss factor were measured with a 1500N force from a large force hammer.*

| **Mass-spring system** | **Resilient material** | **Resilient material thickness (mm)** | **Dynamic stiffness per unit area (MN/m$^3$)** | **ILF (-)** | **Mass-spring frequency (Hz)** |
|---|---|---|---|---|---|
| **A** | Yellow Sylomer | 15 | 23.5 | 0.37 | 62 |
| **B** | Green Sylomer | 15 | 32.6 | 0.32 | 73 |
| **C** | EPS (1) | 20 | 41.1 | 0.62 | 82 |
| **D** | EPS (2) | 25 | 100.2 | 0.41 | 128 |

## 4. IMPACT SOUND INSULATION MEASUREMENT

In test facility A, two measurements with rubber ball excitation were carried out with and without five different mass-spring systems on the base floor. Five different excitation positions were used on the base floor with three accelerometers (B&K, Type 4371) fixed to the floor at random positions for each excitation position. Two microphones (B&K, Type 4165) were used in the receiving room to measure the sound pressure at random positions for each excitation position. B&K Time Data Recorder was used with a time resolution of 61.04μs and an FFT frequency resolution of 1Hz.

In test facility B, two measurements on the floating floor were carried out in with excitation using (a) the rubber ball and (b) the tyre source. Four randomly chosen excitation positions were used on the floating floor with three accelerometers (B&K, Type 4371) fixed to the base floor at random positions for each excitation position, two microphones (B&K, Type 4165) were used in the receiving room to measure the sound pressure at random positions for each excitation position. B&K Pulse was used with a time resolution of 61.04μs and an FFT frequency resolution of 1Hz. In both measurements, the procedures for the rubber ball described in ISO 10140-3:2010 [12] were followed.

## 5. COMPARISON BETWEEN TEST RESULTS AND TSEA PREDICTION

For the TSEA model of test facility A, the CLF from the floor to the room was calculated from the radiation efficiency that was estimated from a previous measurement [9] of the normalised impact sound pressure level with excitation from the ISO tapping machine measurement. The CLF in the reverse direction was determined using the consistency relationship. The predicted results were compared with one-third octave and octave band measurements.

For test facility B, the CLF from the floor to the room was calculated from the frequency-average radiation efficiency from Leppington [10-13]. The CLF in the reverse direction was determined using the consistency relationship. For both facilities the TLF for the concrete base floor was estimated from the sum of all CLFs and the ILF in the TSEA model. The predicted results were compared with measured octave and octave band results.

Figures 3 and 4 show measured and predicted $L_{p,Fmax}$ in test facility A with and without the locally reacting mass-spring systems in one-third octave bands and octave bands. In those figures, the frequency range that is shown in the plot depends on the effectiveness of each mass-spring system or floating floor such that results are only shown when there is a measurable signal that is 10dB above background noise. The maximum difference in $L_{p,Fmax}$ between measurement and TSEA ranged from 5.3 to 8.3dB, and 6.0 to 7.0dB when using $W'_{in,Force\_Plate}$ and $W'_{in,ITSEA}$ respectively in one-third octave bands, and the maximum difference in $L_{p,Fmax}$ between measurement and TSEA ranged from 2.1 to 7.5dB, and 2.0 to 6.0 dB when using $W'_{in,Force\_Plate}$ and $W'_{in,ITSEA}$ respectively in octave bands. In general, the measurement and $L_{p,Fmax}$ predicted with TSEA using $W'_{in,ITSEA}$, have peaks and troughs occurring in the same frequency bands.

Figure 5 shows the comparison of the $L_{p,Fmax}$ for the rubber ball and tyre source dropping on the floating floor on the 210mm base floor. in octave bands there is a difference of over 10dB in $L_{p,Fmax}$ in the 31.5 and 63Hz octave bands. This is likely to be due to an overestimation of the CLF between the concrete slab and the room. An underestimation of $L_{p,Fmax}$ occurs with both excitation sources in the 500Hz octave bands. This may be due to the underestimation of $W'_{in}$.

Table 4 shows the frequency-average difference between measurement and TSEA over all one-third octave bands from 50 Hz up to the maximum frequency band shown in the figure. These differences are considered to be acceptable because (1) the general trend of the measurement and TSEA values are similar; they overlap and cross over each other, and (2) the 95% confidence intervals in the measurement overalap the predicted curves. Therefore, the frequency-average difference in $L_{p,Fmax}$ between measurement and TSEA using $W'_{in,ITSEA}$ of 3.7dB in one-third octave bands and 2.7dB in octave bands is considered as an acceptable difference. This confirms that ITSEA can be used to predict the normalised transient power input with and without locally reacting mass-spring system, and can be used in the TSEA model to incorporate the locally reacting mass-spring systems.

Table 5 shows the frequency-average difference between measurement and TSEA over all octave bands from 31.5 to 250Hz. This shows that there is reasonable agreement (i.e. <5dB) between measurement and TSEA because the aforementioned overestimation and underestimation partly cancel each other out.

The larger differences between measurements and TSEA tend to occur below 100 Hz. To improve the prediction model in this region where the sound field is highly modal and the concrete floors have only a few modes it might be beneficial for future work to consider using a normal mode approach to predict the radiation efficiency [14]. Another issue that is relevant to measurements in modal sound fields is the sampling of the sound pressure in the room which can benefit from using corner microphone positions [15].

The general trend of the measurement and TSEA $L_{p,Fmax}$ above 125Hz octave bands are similar; they overlap and cross over each other. This confirms that ITSEA can be used with two different excitation sources, (rubber ball and tyre source) to predict the normalised transient power input with and without the Ondol floating floor. It also confirms that ITSEA can be used to provide input data for TSEA models to incorporate the floating floor and different excitation sources.

*Table 4. Frequency-average difference between measurement and TSEA for $L_{p,Fmax}$ using one-third octave or octave band data for test facility A.*

| | | | Locally reacting mass-spring systems | | | | |
|---|---|---|---|---|---|---|---|
| | **Transient power input** | **140mm** | **A** | **B** | **C** | **D** | **E** |
| $L_{p,Fmax}$ (dB) | **Force Plate (1/3 octave)** | -2.6 | -4.1 | -1.8 | -0.5 | -1 | -1.1 |
| | **ITSEA (1/3 octave)** | -2 | -1.3 | -3.7 | -2.4 | -0.7 | -2.1 |
| | ***Force Plate (octave)*** | 2.3 | -1.2 | 2.6 | 3.5 | 2.9 | 3.3 |
| | ***ITSEA*(octave)** | -0.7 | 1.2 | -2.7 | -1 | 0.6 | 0.1 |

*Table 5. Frequency-average difference between measurement and TSEA for $L_{p,Fmax}$ using octave band data for test facility B*

| | **Rubber Ball** | **Tyre source** | **Rubber ball (Floating floor)** | **Tyre source (Floating floor)** |
|---|---|---|---|---|
| $L_{p,Fmax}$ (dB) | -3.7 | -2.5 | -3.2 | -2.6 |

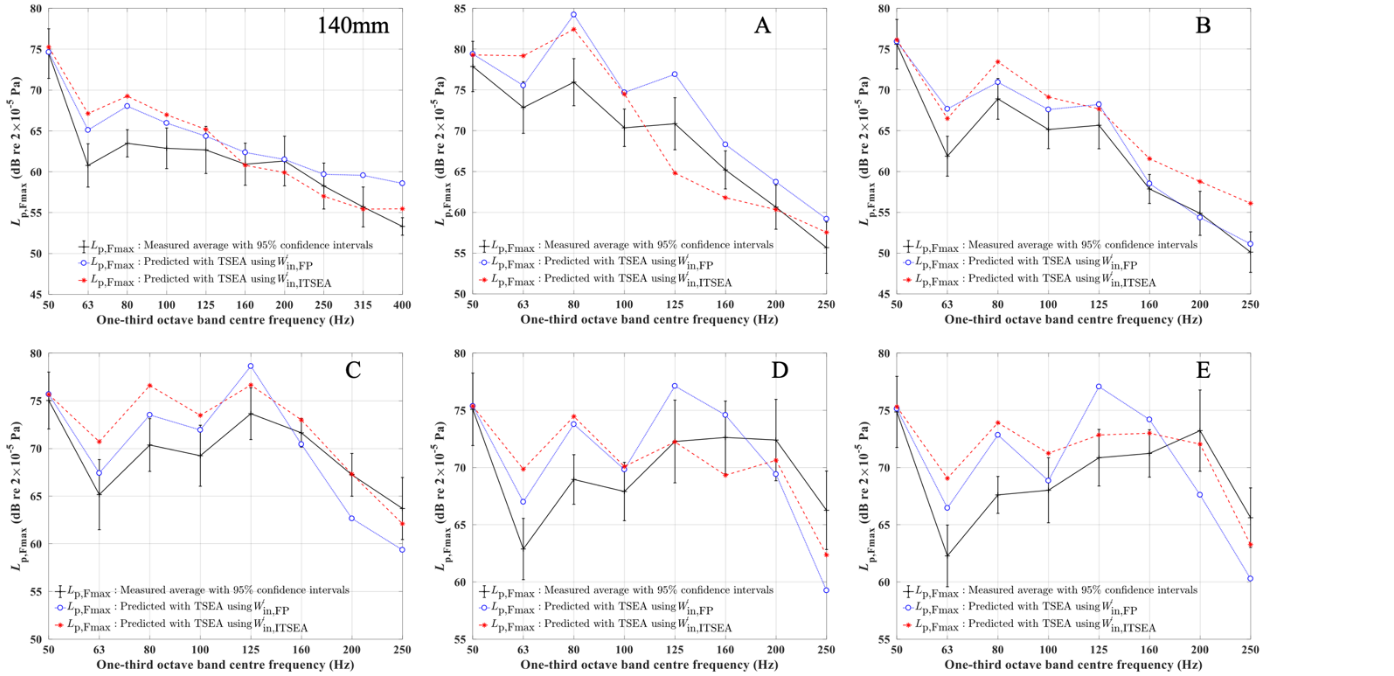


*Figure 3. Comparison of measured and predicted $L_{p,Fmax}$ (one-third octave bands) in test facility A: 140mm bare concrete slab (upper-left), locally reacting mass-spring system A (upper-middle), locally reacting mass-spring system B (upper-right), locally reacting mass-spring system C (lower-left), locally reacting mass-spring system D (lower-middle) , locally reacting mass-spring system E (lower-right).*

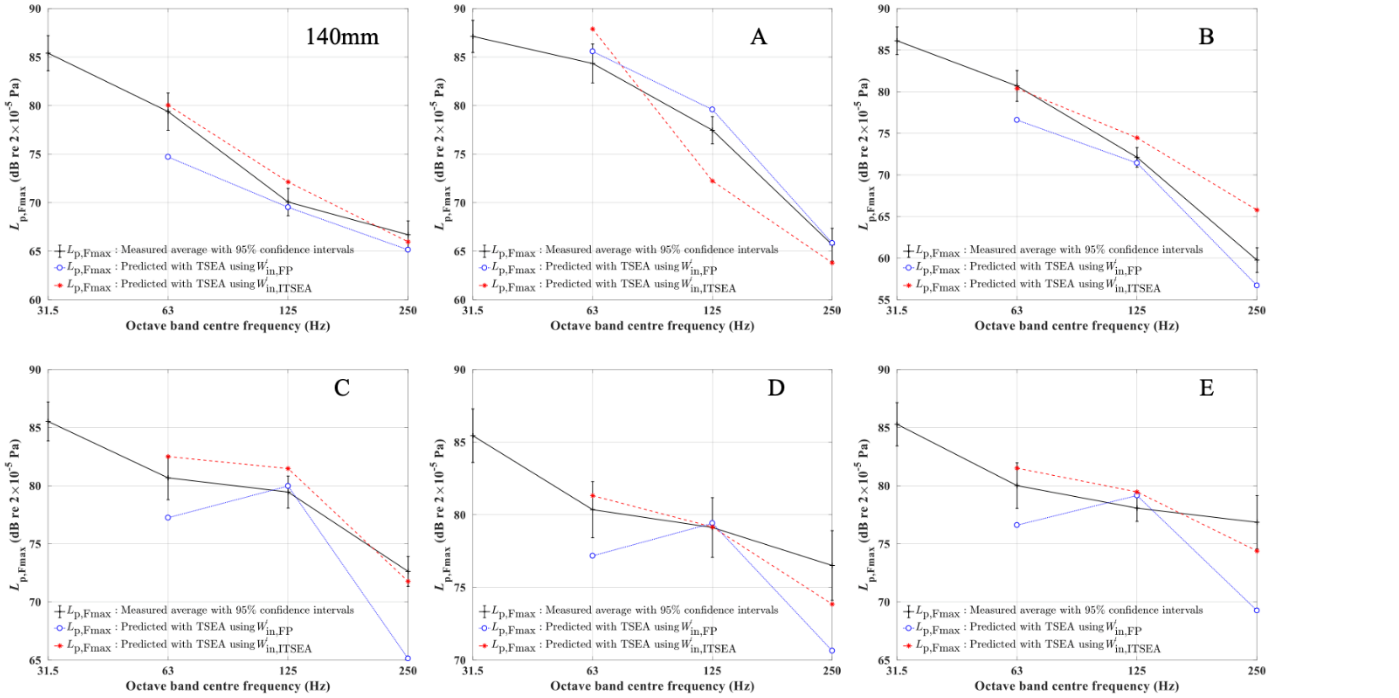


*Figure 4. Comparison of measured and predicted $L_{p,Fmax}$ (octave bands) in test facility A: 140mm bare concrete slab (upper-left), locally reacting mass-spring system A (upper-middle), locally reacting mass-spring system B (upper-right), locally reacting mass-spring system C (lower-left), locally reacting mass-spring system D (lower-middle) , locally reacting mass-spring system E (lower-right).*

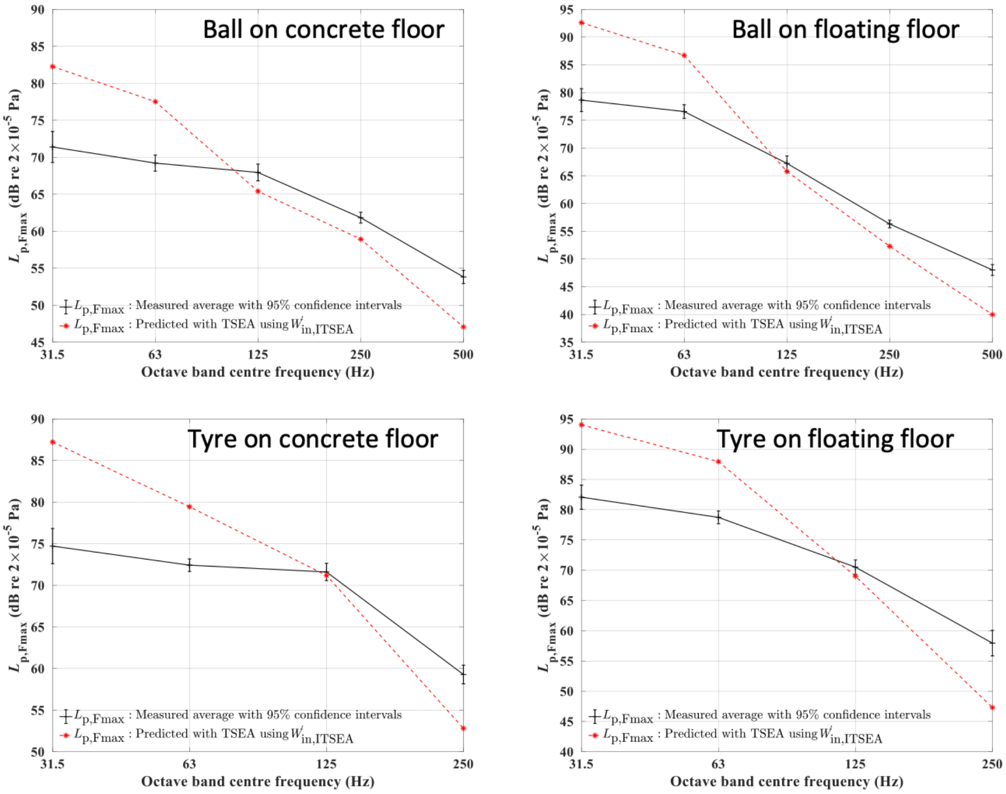


*Figure 5. Comparison of measured and predicted $L_{p,Fmax}$ (octave bands) in test facility B: 210mm bare concrete slab excited by rubber ball (upper-left), floating floor on 210mm concrete slab excited by rubber ball (upper-right), 210mm bare concrete slab excited by tyre source (lower-left), floating floor on 210mm concrete slab excited by tyre source (lower-right).*

## 6. CONCLUSIONS

TSEA models have been developed for a concrete base floor with or without a floating floor that radiates into a receiving room. The normalised transient power input for the model was determined using ITSEA on the base floor and the same base floor with a full-size floating floor as well as force plate measurements on small mass-spring systems representing idealised floating floors. All results showed reasonable agreement (i.e. <5dB in one-third octave or octave bands) with the measured $L_{p,Fmax}$ in the receiving room. This validates the TSEA approach for heavy impact sources such as the rubber ball and bang machine and allows prediction of Fast time-weighted maximum sound pressure levels in heavyweight buildings where the sound transmission is direct and/or flanking transmission.

## 7. ACKNOWLEDGEMENT

The authors gratefully acknowledge the funding for this research which has been carried out at the Acoustics Research Unit at the University of Liverpool with financial support by grants (16REP-B082204-05) and (18REP-B082204-05) from Residential Environment Research Program funded by Ministry of Land, Infrastructure and Transport of Korean Government. For assistance with the measurements, the author is grateful to Dr Byung Kwon Lee for providing access to the LH laboratory in Korea and collecting the raw time domain data for the Ondol floating floor, to Gary Timmins for providing access to the BRE laboratory and Dr. Gary Seiffert for assisting with the transmission suite measurements at BRE.

Dr Hirakawa is grateful for management expense grants from the Building Research Institute for this conference paper.

## 8. REFERENCES


1. EN ISO 10140-3:2010+A1:2015. Acoustics – Laboratory measurement of sound insulation of building elements – Part 3: Measurement of impact sound insulation. International Organization for Standardization.
2. EN ISO 10140-5:2010+A1:2014. Acoustics – Laboratory measurement of sound insulation of building elements – Part 5: Requirements for test facilities and equipment. International Organization for Standardization.
3. JIS A 1418-2: 2000. Acoustics – Measurement of floor impact sound insulation of buildings – Part 2: Method using standard heavy impact source, Japanese Industrial Standards Committee, 2000.
4. KS F 2810-2:2001. Method for field measurement of floor impact sound insulation. Part 2: Method using standard heavy impact sources. Korean Standard Committee, South Korea, 2001.
5. Robinson M and Hopkins C. Prediction of maximum time-weighted sound and vibration levels using transient statistical energy analysis. Part 1: Theory and numerical implementation. Acta Acust united Ac 2014;100(1):46–56.
6. Robinson M and Hopkins C. Prediction of maximum time-weighted sound and vibration levels using transient statistical energy analysis. Part 2: Experimental validation. Acta Acust united Ac 2014;100(1):57–66.
7. Robinson M and Hopkins C. Prediction of maximum fast time-weighted sound pressure levels due to transient excitation from the rubber ball and human footsteps. Build Environ 2015; 94:810–20.
8. Hirakawa S. Hopkins C. Experimental determination of transient structure-borne sound power from heavy impact sources on heavyweight floors with floating floor using an inverse form of transient statistical energy analysis, Appl. Acoust., 2018;140.74-82. doi: 10.1016/j.apacoust.2018.05.020
9. Hopkins C. Sound Insulation, 1st ed., Butterworth-Heinemann, Oxford, UK, 2007. doi:10.4324/9780080550473.
10. Leppington F.G, Broadbent E.G, Heron K.H, The Acoustic Radiation Efficiency of Rectangular Panels, Proc. R. Soc. A Math. Phys. Eng. Sci. 382A, 1982 245–271. doi:10.1098/rspa.1982.0100.
11. Leppington F.G, Broadbent E.G, Heron K.H, Acoustic Radiation from Rectangular Panels with Constrained Edges, Proc. R. Soc. A Math. Phys. Eng. Sci. A393, 1984 67–84. doi:10.1098/rspa.1984.0046.
12. Leppington F.G, Heron K.H, Broadbent E.G, Mead S.M, Resonant and Non-Resonant Acoustic Properties of Elastic Panels. II. The Transmission Problem, Proc. R. Soc. A Math. Phys. Eng. Sci. 412, 1987, 309–337. doi:10.1098/rspa.1987.0091.
13. Leppington F.G, Acoustic radiation from plates into a wedge-shaped fluid region: application to the free plate problem, Proc. R. Soc. London. 452 (1996) 1745–1764. doi:10.1098/rspa.1996.0093.
14. Hopkins, C., Filippoupolitis, M. and Ferreira, N, 2015. Prediction of low-frequency radiation efficiencies using the normal mode approach and finite element methods. In Proceedings of the 22nd International Congress on Sound and Vibration.
15. Hirakawa, S., Hopkins, C. and Lee, P.J, 2018. Comparison and assessment of Japanese, Korean and international measurement procedures for impact sound insulation with heavy impact sources. In Proceedings of the 25th International Congress on Sound and Vibration.